International Journal on Emerging Technologies 11(2): 1054-1060(2020)
ISSN No. (Print): 0975-8364
ISSN No. (Online): 2249-3255

Characteristics of Double-porous Layered Slider Bearing with Parabolic Pad Stator using Ferrofluid Lubricant

Darshana A. Patel[1] and Ramesh C. Kataria[2]
[1]Assistant Professor, Department of Mathematics and Humanities,
Vishwakarma Government Engineering College, Ahmedabad (Gujarat), India.
[2]Assistant Professor, Department of Mathematics,
Som-Lalit Institute of Computer Applications, Ahmedabad (Gujarat), India.

(Corresponding author: Ramesh C. Kataria)
(Received 02 March 2020, Revised 09 April 2020, Accepted 11 April 2020)
(Published by Research Trend, Website: www.researchtrend.net)

ABSTRACT: A mathematical analysis of ferrohydrodynamics lubrication in a slider bearing having a parabolic pad stator with a double porous layered slider which is backed by the solid wall has been presented considering the effect of slip velocity at the film-porous boundary as proposed by Sparrow et al. [14]. The study includes squeeze velocity and variable magnetic field, which is applied obliquely. Modified Reynolds-type equation is derived using the model suggested by Neuringer-Rosensweig with the continuity equation. Non-dimensional film pressure and load-carrying capacity equations have been derived. It is observed in the analysis that, non-dimensional film pressure increased with increasing values of the field strength. Also, it is observed that for the different sizes of the porous regions and different permeabilities, the values of non-dimensional load-carrying capacity are evaluated at various parametric conditions and represented in the graphical and tabular forms. The graph indicates that non-dimensional load-carrying capacity increased when the non-dimensional magnetization parameter increased whereas the slip parameter decreased. After analyzing the model, it was found that when we interchange the values of k_1 and k_2 for both $dh/dt=0$ and $dh/dt\neq 0$, load-carrying capacity increases significantly as compared to the model suggested by Shah and Kataria [21].

Keywords: Double porous layered slider bearing, Ferrohydrodynamics lubrication, slip velocity, squeeze velocity.

NOMENCLATURE

a	h_1/h_0
A	Bearing length
B	Bearing breadth
d	Difference between inlet and outlet film thickness
l_1, l_2	Widths of the porous regions (m)
h	Fluid film thickness (m)
$\bar{h}$	Non-dimensional film thickness (h / h_1)
h_1, h_2	Minimum and maximum values of h (m)
dh/dt	Squeeze velocity (m/s)
H	Strength of variable magnetic field (A / m)
$\vec{\mathrm{H}}$	Magnetic field vector
K	Quantity as defined in eq. (2) (A^2 / m^4)
k_1, k_2	Permeability of the porous regions (m^2)
$\vec{\mathrm{M}}$	Magnetization vector
p	Film pressure (N / m^2)
P	Fluid pressure in the porous matrix (N / m^2)
$\vec{V}$	Fluid velocity vector
s	Slip parameter (1 /m)
$\bar{s}$	Non-dimensional slip parameter
t	Time (s)
u, v, w	Components of film fluid velocity in x, y and z –directions (m/s)
U	Velocity of slider (m/s)
u_i', w_i'	Darcy's velocity components in the x and z -directions respectively
W	Load-carrying capacity (N)
$\overline{W}$	Non-dimensional load-carrying capacity as defined in eq. (34)
x, y, z	Cartesian co-ordinates (m)
	Greek symbols
ξ	Fluid viscosity (N s / m^2)
μ_0	Free space permeability (N / A^2)
α	Slip constant
ρ	Fluid density (N s^2 /m^4)
$\bar{\mu}$	Magnetic susceptibility
μ^*	Non-dimensional magnetization parameter as defined in eq. (28)
δ	Profile parameter

I. INTRODUCTION

Due to the self-lubricated nature and low price, porous bearings have been widely used in industries such as in instruments, automobiles, domestic appliances, small electric motors, and machines. Porous bearings have a self-contained oil reservoir therefore there is no requirement of external lubricant supply for the whole life of the machine. Initially, the systematic study of porous bearings has been carried out by Morgan and Cameron [1] and suggested solution for short bearing, several other researchers [2-5] have proposed the use of a variety of porous bearings and shown that effect of porosity decreases load carrying capacity and friction force.

To eliminate these flaws, ferrofluid can be used as a lubricant. Ferrofluid [6] is a colloidal dispersion containing fine ferromagnetic particles, like ferric oxide in a non-conducting carrier liquid. In a carrier liquid suitable surfactant is added to generate coating layer to prevent flocculation of the particles. Usually, ferrofluid contains approximately 85% carrier liquid, 10% surfactant, and 5% magnetic solids. By the external application of a magnetic field, ferrofluid experiences magnetic body forces. There are many advantages of using ferrofluid as a lubricant, like ferrofluids are retained at the desired location, no rubbing takes place between solid materials, no external lubrication is required, and no side leakage is possible. Consequently, ferrofluids are helpful in many applications like in sealing, in cooling and heating cycles, in high sliding speeds, in sensors, in elastic damper, etc. [7-10].

Agrawal [11] studied effects of ferrofluid on inclined porous slider bearing and concluded that the load - carrying capacity increases with increase in Magnetization parameter. Prajapati [12] studied porous squeeze film bearings with ferrofluid and confirmed that load-carrying capacity increases as magnetization parameter increases. Ram *et al.* [13] presented performance of three-layered porous squeeze film bearing under the application of ferrofluid and concluded that in the presence of magnetic fluid, load carrying capacity increases significantly.

Researchers [1-13] took the usual assumptions related to noslip condition at film- porous interface. The results presented by Sparrow *et al.,* [14] shows, porous media plays an effective role in shrinking the response time of squeeze films. Especially, the faster response can be attained by the use of porous materials which draw attention to velocity slip. Prakash and Vij [15] analysed narrow porous journal bearing with the help of Beavers – Joseph condition of velocity slip and results were compared with earlier results obtained using no-slip condition. Patel and Gupta [16] studied a porous inclined slider bearing with slip velocity at the interface of film-porous interface and found that minimization of the slip parameter is crucial to increase the load capacity. Shah and Bhat [17] analyzed that load and center of pressure remain unaffected when the slip parameter increased, whereas for high material parameter values, center of pressure shifting towards the inlet of bearing and no change in load. Ahmed and Singh [18] studied ferrofluid lubrication in porous pivoted slider with velocity slip and the result showed that load capacity increases as the magnetic parameter increases simultaneously it decreases as the slip parameter and permeability parameter increases. Shah *et al.,* [19] theoretically studied inclined porous slider bearing assuming slip velocity. Shah and Patel [20] studied ferromagnetic lubrication on double porous layered axially undefined journal bearing taking into consideration of anisotropic permeability with respect to porous layer and slip velocity at the surface of the porous layer. Recently, Shah and Kataria [21] analyzed slider bearing having convex pad stator and double porous layers attached to the slider using the ferrofluid model suggested by Neuringer-Rosensweig. Subsequently, researchers [22-25] have also analyzed the effects of ferrofluids in their study from different perspectives.

The present investigation is concerned with the study of ferromagnetic lubrication slider bearing having a parabolic pad stator. Double porous layered attached to the slider under the presence of a variable magnetic field oblique to the lower surface. The flow of lubricant through porous regions follows Darcy law. As a result, the present study established a suitable Reynolds equation. Equations for non-dimensional film pressure distribution and load capacity are derived and evaluated numerical results at various parametric conditions are represented in the graphical form.

II. ANALYSIS

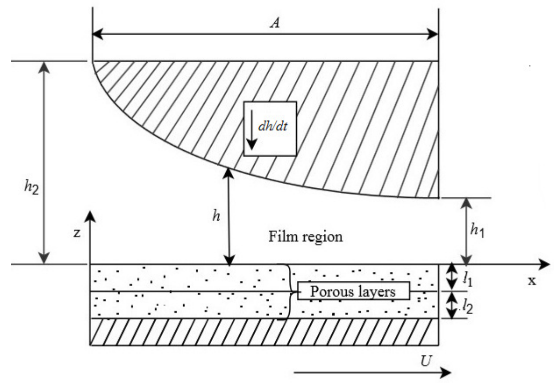

Fig. 1. Double-porous layered slider bearing with parabolic pad surface.

Fig. 1 shows the geometry of the system under study. The upper surface -parabolic pad stator and lower surface-slider is moving in the *x*-direction with a uniform velocity *U*. The gap between two lubricating surfaces, slider and stator is known as the fluid-film region, called film thickness. It is assumed that the region is filled with water –based ferrofluid lubricant.

***Modified Reynolds Equation*:**

Film thickness *h* [26], in this case can be represented by

$$h = h_1 + \frac{d}{A}\left(A - 2x + \frac{x^2}{A}\right), 0 \le x \le A, \tag{1}$$

Here, h_1 and h_2 are minimum and maximum film thickness at the outlet and inlet respectively, and *d* denotes difference between the inlet and the outlet film thickness.

The lower surface-slider is attached with two porous layers of widths l_2 and l_1, porous layer of width l_2 is attached first and then of width l_1. Also, the stator moves towards the lower surface-slider with the velocity dh/dt , is called squeeze velocity.

Oblique magnetic field [21] applied to the lower surface is defined as

$$H^2 = K\, x(A - x), \tag{2}$$

where *K* is a quantity taken to match both sides dimensions of the equation. Using which maximum magnetic field strength is at $x = A/2$, as follows from [21]. From equation (2), Max. $H^2 = 10^{-4} K$ which implies for $K = O(10^{10})$, so that $H = O(10^3)$ or $O(\mathrm{H}) \approx 3,$ where *O* indicates order.

The equations governing the motion of ferrofluid [6] with continuity equation are given by *Equation of Motion*:

$$\rho\left[\frac{\partial\vec{V}}{\partial t}+\left(\vec{V}\bullet\vec{\nabla}\right)\vec{V}\right]=-\vec{\nabla}p+\xi\,\nabla^2\vec{V}+\mu_0(\vec{\mathrm{M}}\bullet\vec{\nabla})\vec{\mathrm{H}} \tag{3}$$

where $\vec{V}=(u,\ v,\ w)$ is the fluid velocity field, p is the film pressure, ρ and ξ are the density and viscosity of the fluid, μ_0 is the permeability of free space, magnetization $\vec{\mathrm{M}}$ and magnetic field $\vec{\mathrm{H}}$.

Continuity Equation:

$$\vec{\nabla}\bullet\vec{V}=0, \tag{4}$$

Where, velocity components of film fluid are u, v,w in x, y and z –directions respectively.

Equations of Electromagnetic Field:

$$\vec{\nabla}\times\vec{\mathrm{H}}=0, \tag{5}$$

$$\vec{\mathrm{M}}=\bar{\mu}\,\vec{\mathrm{H}}, \tag{6}$$

$$\vec{\nabla}\bullet\left(\vec{\mathrm{H}}+\vec{\mathrm{M}}\right)=0, \tag{7}$$

where $\bar{\mu}$ is the magnetic susceptibility.

Using equations (3) to (7) and with the usual assumptions of the theory of hydrodynamics lubrication [27]; for the ferrohydrodynamics lubrication, governing pressure profile in the film region is given by

$$\frac{\partial}{\partial z}\left(\xi\,\frac{\partial u}{\partial z}\right)=\frac{\partial}{\partial x}\left(p-\frac{1}{2}\mu_0\bar{\mu}\mathrm{H}^2\right), \tag{8}$$

where H is the magnetic field strength.

Slip boundary conditions with the addition of slider velocity U for the film region are given by Sparrow *et al.* [14],

$$u=\frac{1}{s}\frac{\partial u}{\partial z}+U\ ;\quad s=\frac{\alpha}{\sqrt{k_1}},\ \text{at}\ z=0\ \text{and} \tag{9}$$

$$u=0,\ \text{at}\ z=h. \tag{10}$$

Equation (8), together with boundary conditions (9) and (10), is solved to yield

$$u=\frac{(h-z)s}{(1+sh)}U+\left\{\frac{(z+h+shz)(z-h)}{2\xi(1+sh)}\right\}\frac{\partial}{\partial x}\left(p-\frac{1}{2}\mu_0\bar{\mu}\mathrm{H}^2\right), \tag{11}$$

Where s: slip parameter, α: slip coefficient and k_1: permeability of the upper porous layer. All depends on the characteristics of the porous material and independent on the lubricant properties and film thickness.

Integrating equation (11) over the film thickness, yields

$$\int_0^h u\,dz=\frac{sh^2}{2(1+sh)}U-\frac{h^3(4+sh)}{12\xi(1+sh)}\frac{\partial}{\partial x}\left(p-\frac{1}{2}\mu_0\bar{\mu}\mathrm{H}^2\right). \tag{12}$$

Continuity equation in the integral form for the film region is given by

$$\frac{\partial}{\partial x}\int_0^h u\,dz+w_h-w_0=0, \tag{13}$$

Using equation (12), equation (13) reduces to

$$\frac{\partial}{\partial x}\left\{\frac{sh^2}{2(1+sh)}U-\frac{h^3(4+sh)}{12\xi(1+sh)}\frac{\partial}{\partial x}\left(p-\frac{1}{2}\mu_0\bar{\mu}\mathrm{H}^2\right)\right\}=w_0+dh/dt, \tag{14}$$

where $w\big|_{z=h}=w_h=-\,dh/dt$, which represents the effect of squeeze velocity in the downward z- direction. And, $w\big|_{z=0}=w_0$.

The velocity components in x, z -directions in the porous region are obtained from Darcy's law are

$$u_i'=\frac{-k_i}{\xi}\frac{\partial}{\partial x}\left(P_i-\frac{1}{2}\mu_0\bar{\mu}\mathrm{H}^2\right) \tag{15}$$

$$w_i'=\frac{-k_i}{\xi}\frac{\partial}{\partial z}\left(P_i-\frac{1}{2}\mu_0\bar{\mu}\mathrm{H}^2\right) \tag{16}$$

where i = 1, 2 represents index of velocity components in the porous regions of widths l_1 and l_2 respectively with permeabilities as k_1 and k_2. Also, P_1 and P_2 indicates fluid pressure of upper and lower porous regions respectively.

Assuming continuity of the flow between two porous layers over z direction, one obtains

$$\left[-\frac{k_1}{\xi}\frac{\partial P_1}{\partial z}+\frac{\mu_0\bar{\mu}k_1}{2\xi}\frac{\partial\mathrm{H}^2}{\partial z}\right]_{z=-l_1}=\left[-\frac{k_2}{\xi}\frac{\partial P_2}{\partial z}+\frac{\mu_0\bar{\mu}k_2}{2\xi}\frac{\partial\mathrm{H}^2}{\partial z}\right]_{z=-l_1}. \tag{17}$$

Also, at impermeable lower plate surface

$$\left[-\frac{k_2}{\xi}\frac{\partial P_2}{\partial z}+\frac{\mu_0\bar{\mu}k_2}{2\xi}\frac{\partial\mathrm{H}^2}{\partial z}\right]_{z=-(l_1+l_2)}=0. \tag{18}$$

The equation of continuity in the porous region is given by

$$\frac{\partial u'}{\partial x}+\frac{\partial w'}{\partial z}=0, \tag{19}$$

substituting equations (15) and (16) into equation (19), one obtains

$$\frac{\partial^2}{\partial x^2}\left(P_i-\frac{1}{2}\mu_0\bar{\mu}\mathrm{H}^2\right)+\frac{\partial^2}{\partial z^2}\left(P_i-\frac{1}{2}\mu_0\bar{\mu}\mathrm{H}^2\right)=0,$$

where i = 1, 2. (20)

Integrating equation (20) w. r. to z across the upper porous layer $(-l_1,\ 0)$, yields

$$\frac{\partial}{\partial z}(P_1-\frac{1}{2}\mu_0\bar{\mu}\mathrm{H}^2)\Big|_{z=0}-\frac{\partial}{\partial z}(P_1-\frac{1}{2}\mu_0\bar{\mu}\mathrm{H}^2)\Big|_{z=-l_1}$$
$$=-\int_{-l_1}^{0}\frac{\partial^2}{\partial x^2}(P_1-\frac{1}{2}\mu_0\bar{\mu}\mathrm{H}^2)dz$$
$$=-l_1\frac{\partial^2}{\partial x^2}(P_1-\frac{1}{2}\mu_0\bar{\mu}\mathrm{H}^2) \tag{21}$$

Again, integrating equation (20) w. r. to z across the lower porous layer $(-(l_1+l_2),\ -l_1)$, yields

$$\frac{\partial}{\partial z}\left(P_2-\frac{1}{2}\mu_0\bar{\mu}\mathrm{H}^2\right)\Big|_{z=-l_1}-\frac{\partial}{\partial z}\left(P_2-\frac{1}{2}\mu_0\bar{\mu}\mathrm{H}^2\right)\Big|_{z=-(l_1+l_2)}$$

$$=-\int_{-(l_1+l_2)}^{-l_1}\frac{\partial^2}{\partial x^2}\left(P_2-\frac{1}{2}\mu_0\bar{\mu}\mathrm{H}^2\right)dz \tag{22}$$

$$=-l_2\frac{\partial^2}{\partial x^2}\left(P_2-\frac{1}{2}\mu_0\bar{\mu}\mathrm{H}^2\right)$$

Using condition (17), equation (21) becomes

$$\frac{\partial}{\partial z}\left(P_1-\frac{1}{2}\mu_0\bar{\mu}\mathrm{H}^2\right)\Big|_{z=0}$$

$$=-l_1\frac{\partial^2}{\partial x^2}\left(P_1-\frac{1}{2}\mu_0\bar{\mu}\mathrm{H}^2\right)+\frac{k_2}{k_1}\frac{\partial}{\partial z}\left(P_2-\frac{1}{2}\mu_0\bar{\mu}\mathrm{H}^2\right)\Big|_{z=-l_1} \tag{23}$$

Substituting equations (18) and (22) in the equation (23) and making use of Morgan-Cameron approximation [24], yields

$$\left[\frac{\partial}{\partial z}\left(P_1-\frac{1}{2}\mu_0\bar{\mu}\mathrm{H}^2\right)\right]_{z=0} \tag{24}$$

$$=-\left(\frac{k_1l_1+k_2l_2}{k_1}\right)\frac{d^2}{dx^2}\left(p-\frac{1}{2}\mu_0\bar{\mu}\mathrm{H}^2\right).$$

At the film-porous interface the velocity component in z-direction must be continuous, therefore,

$$w\big|_{z=0}=w'\big|_{z=0}=\left[\frac{-k_1}{\xi}\frac{\partial}{\partial z}\left(P_1-\frac{1}{2}\mu_0\bar{\mu}\mathrm{H}^2\right)\right]_{z=0} \tag{25}$$

Substituting equation (25) into equation (14) gives

$$\left[\frac{-k_1}{\xi}\frac{\partial}{\partial z}\left(P_1-\frac{1}{2}\mu_0\bar{\mu}\mathrm{H}^2\right)\right]_{z=0}$$

$$=-dh/dt+\frac{\partial}{\partial x}\left\{\frac{sh^2U}{2(1+sh)}-\frac{h^3(4+sh)}{12\xi(1+sh)}\frac{\partial}{\partial x}\left(P-\frac{1}{2}\mu_0\bar{\mu}\mathrm{H}^2\right)\right\}. \tag{26}$$

Using equation (24), (26) and the fact that $\frac{\partial H^2}{\partial z}=0$, equation (14) transforms to

$$\frac{d}{dx}\left[\left\{12\left(k_1l_1+k_2l_2\right)+\frac{h^3(4+sh)}{(1+sh)}\right\}\frac{d}{dx}\left(p-\frac{1}{2}\mu_0\bar{\mu}\mathrm{H}^2\right)\right] \tag{27}$$

$$=-12\xi dh/dt+6\xi U\frac{d}{dx}\left(\frac{sh^2}{1+sh}\right).$$

Equation (27) is modified Reynolds equation.

Non- dimensionalisation

By the following substitutions

$$X=\frac{x}{A},\ \bar{h}=\frac{h}{h_0},\ \bar{s}=s\,h_0,\ \bar{p}=\frac{h_0^2\,p}{\xi UA},\ S=\frac{2A\,dh/dt}{U\,h_0},$$

$$\mu^*=\frac{\mu_0\bar{\mu}\,KAh_0^2}{\xi U},\ \psi=\frac{k_1l_1+k_2l_2}{h_0^3},\ a=\frac{h_1}{h_0},\ \delta=\frac{d}{h_0}. \tag{28}$$

The non-dimensional forms of equation (27) is as follows

$$\frac{d}{dX}\left[G\frac{d}{dX}\left\{\bar{p}-\frac{1}{2}\mu^*X(1-X)\right\}\right]=\frac{dE}{dX}, \tag{29}$$

Here $G=12\psi+\frac{\bar{h}^3(4+\bar{s}\bar{h})}{(1+\bar{s}\bar{h})}$, $E=\frac{6\bar{s}\bar{h}^2}{(1+\bar{s}\bar{h})}-6SX$.

The film thickness h in non-dimensional form as

$$\bar{h}=a+\delta(1-2X+X^2) \tag{30}$$

Further, non-dimensional form of the magnetic field H defined in equation (2) is

$$\mathrm{H}^2=KA^2X(1-X). \tag{31}$$

***Pressure Distribution*:**

Solving equation (29), together with pressure boundary conditions

$$\bar{p}=0 \text{ at } X=0 \text{ and } X=1 \tag{32}$$

gives, the film pressure $\bar{p}$ in non-dimensional form as

$$\bar{p}=\frac{1}{2}\mu^*X(1-X)+\int_0^X\frac{E-F}{G}dX,$$

$$\text{Where } F=\int_0^1\frac{E}{G}dX\Big/\int_0^1\frac{1}{G}dX. \tag{33}$$

***Load Capacity*:**

The non-dimensional load carrying capacity $\bar{W}$ can be derived as follows

$$\bar{W}=\frac{Wh_1^2}{B\xi UA^2}=\frac{\mu^*}{12}-\int_0^1\frac{E-F}{G}X\,dX,$$

$$\text{where } w=\int_0^B\int_0^A p\,dx\,dy. \tag{34}$$

III. RESULTS AND DISCUSSION

Non-dimensional load capacity is numerically calculated from equation (34) for the following values of the different parameters [21]. For the calculations, Simpson's 1/3 – rule for step size 0.1 is used.

$h_1=0.05\,(m),\ h_2=0.10\,(m),\ U=1\ (ms^{-1}),\ A=0.15\ (m),$

$\bar{\mu}=0.05,\ h_0=0.05\,(m),\ dh/dt=0.005\ (ms^{-1}),$

$\xi=0.012\ (\mathrm{Nsm^{-2}}),\ K=10^9,\ \mu_0=4\pi\times10^{-7}(\mathrm{NA^{-2}}),$

$l_i=0.01\,(m),\ \alpha=0.1.$

Discussion on non-dimensional film pressure

Graphical demonstration of the results obtained for pressure profile $\bar{p}$ for the values of non-dimensional parameter X is shown below

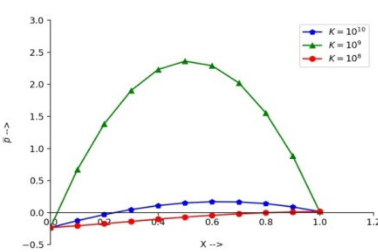

Fig. 2 Non-dimensional pressure versus non-dimensional parameter X

Table 1: $\bar{p}$ verses X for different values of δ considering K=10^{10}

δ	$\bar{p}$				
	X=0.2	X=0.4	X=0.6	X=0.8	X=1.0
0.6	1.4182538	2.2418637	2.2849028	1.5394568	0.0014452
0.8	1.3979529	2.2345927	2.2875736	1.5470539	0.0098454
1.0	1.3830551	2.2315147	2.2919836	1.5539194	0.0159159

A plot of non-dimensional pressure $\bar{p}$ for different values of field strength K is shown in Fig. 2. It shows that increase in the field strength K, taking into consideration k_1 = 0.0001, k_2 = 0.0001 and $dh/dt \neq 0$, indicates an increase in the pick pressure.

Table 1 shows that non-dimensional film pressure $\bar{p}$ was little affected by different values of δ and X considering K=10^{10}.

Discussion on non-dimensional load capacity

The calculated values of $\bar{W}$ are presented as below:

Table 2: Effects on $\bar{W}$ for the same values of k_1 and k_2 assuming $dh/dt = 0$ and $dh/dt \neq 0$

k_1	k_2	$\bar{W}$	
		$dh/dt = 0$	$dh/dt \neq 0$
0.0001	0.0001	0.2024584	0.2045595
0.01	0.01	0.1656103	0.1660992
% increase in $\bar{W}$		22.25	23.16

The results for $\bar{W}$ for same values of k_1 and k_2 assuming $dh/dt = 0$ and $dh/dt \neq 0$ are computed and presented in Table 2. It is reveals that, when k_1 = k_2= 0.0001, $\bar{W}$ increases about 23% for both the cases $dh/dt = 0$ and $dh/dt \neq 0$ as compared to k_1 = k_2 = 0.01.

Table 3: Effects on $\bar{W}$ by swapping values of k_1 and k_2 assuming $dh/dt = 0$ and $dh/dt \neq 0$

k_1	k_2	$\bar{W}$	
		$dh/dt = 0$	$dh/dt \neq 0$
0.1	0.0001	0.1638827	0.1640203
0.0001	0.1	0.1667478	0.1668908
% increase in $\bar{W}$		1.75	1.75

Table 3 shows the values of $\bar{W}$ by swapping the values of k_1 and k_2, for two different cases of $dh/dt = 0$ and $dh/dt \neq 0$. It is observed that when k_1 <k_2, $\bar{W}$ increases about 1.75 % in both the cases $dh/dt = 0$ and $dh/dt \neq 0$ as compared to k_1 >k_2.

Table 4 indicates a comparative study of $\bar{W}$, when we swap the widths of the upper and lower porous regions for three different cases of k_1 and k_2(*i.e.* k_1 = k_2,k_1< k_2, k_1> k_2) considering $dh/dt = 0$ and $dh/dt \neq 0$ When k_1 = k_2 = 0.01, $\bar{W}$ remains same for both $dh/dt = 0$ and $dh/dt \neq 0$.

It is observed that when the permeability of the lower porous layer is small as compared to upper porous layer (*i.e.* k_1 = 0.1 and k_2 = 0.0001), $\bar{W}$ increases with the increase of width of lower porous layer as compared to upper porous layer. Also, when k_1 = 0.0001 and k_2 = 0.1, that is permeability of upper porous layer is small as compared to lower porous layer, $\bar{W}$ increases with the increase of width of upper porous layer as compared to lower porous layer.

Table 5 indicates that $\bar{W}$ increases, when size of upper porous layer and lower porous layer are small in all the three cases; that is, for k_1 = k_2, k_1< k_2, k_1> k_2 for both $dh/dt = 0$ and $dh/dt \neq 0$.

It is observed from the Table 6 that with the increase of squeeze velocity $\bar{W}$ increases. Thus, squeeze velocity has an impact on the design of slider bearing.

Table 7 shows the comparative study of conventional lubricant ($\mu^* = 0$) and magnetic fluid ($\mu^* \neq 0$) on $\bar{W}$ by considering two same values of k_1 and k_2 with and without the effect of squeeze velocity. It is noticed that using magnetic fluid as lubricant, $\bar{W}$ increases significantly as compared to conventional lubricant. Also, it is found that when k_1 = k_2 = 0.0001, $\bar{W}$ increases considerably as compared to k_1 = k_2 = 0.01 for conventional as well as magnetic fluid.

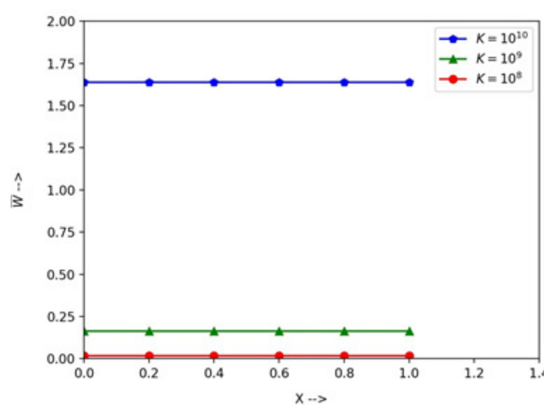

Fig. 3. Non-dimensional load carrying capacity against non-dimensional parameter X.

Fig. 3 shows the variation of non-dimensional load capacity $\bar{W}$ as a function of non-dimensional parameter X for different values of the field strength K considering k_1 = 0.0001 and k_2 = 0.0001 and $dh/dt \neq 0$. It can be observed that $\bar{W}$ considerably increased by increasing K.

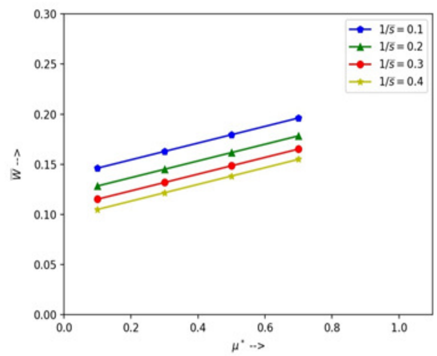

Fig. 4. Non-dimensional load carrying capacity against non-dimensional magnetization parameter.

The variation of non-dimensional load carrying capacity $\overline{W}$ with respect to non-dimensional magnetization parameter μ^* to read influence of non –dimensional slip parameter $1/\overline{s}$ is presented in Fig. 4. It is observed that as non-dimensional slip parameter $1/\overline{s}$ decreases $\overline{W}$ increases. Additionally, $\overline{W}$ increases with increasing values of magnetization parameter μ^* which indicates that under the presence of magnetic fluid bearing performance improved significantly.

Table 4: Values of $\overline{W}$ by swapping values of l_1 and l_2 assuming $dh/dt = 0$ and $dh/dt \neq 0$

l_1	l_2	$\overline{W}$					
		$k_1 = k_2 = 0.01$		$k_1 = 0.1$, $k_2 = 0.0001$		$k_1 = 0.0001$, $k_2 = 0.1$	
		$dh/dt = 0$	$dh/dt \neq 0$	$dh/dt = 0$	$dh/dt \neq 0$	$dh/dt = 0$	$dh/dt \neq 0$
3	1	0.1637069	0.1637108	0.1636912	0.1636918	0.1637242	0.1637257
1	3	0.1637069	0.1637108	0.1636927	0.1636943	0.1637018	0.1637023

Table 5: Values of $\overline{W}$ for same values of l_1 and l_2 assuming $dh/dt = 0$ and $dh/dt \neq 0$

l_1	l_2	$\overline{W}$					
		$k_1 = k_2 = 0.01$		$k_1 = 0.1$, $k_2 = 0.0001$		$k_1 = 0.0001$, $k_2 = 0.1$	
		$dh/dt = 0$	$dh/dt \neq 0$	$dh/dt = 0$	$dh/dt \neq 0$	$dh/dt = 0$	$dh/dt \neq 0$
1	1	0.1637231	0.1637309	0.1636927	0.1636943	0.1637242	0.1637258
3	3	0.1637014	0.1637040	0.1636912	0.1636918	0.1637018	0.1637023

Table 6: Effect of squeeze velocity on $\overline{W}$ considering $k_1 = k_2 = 0.0001$

dh/dt	0.00	0.001	0.002	0.003	0.004	0.005
$\overline{W}$	0.2024584	0.2028786	0.2032988	0.2037190	0.2041392	0.2045595

Table 7: Comparative study of conventional lubricant ($\mu^* = 0$) and magnetic fluid ($\mu^* \neq 0$) on $\overline{W}$ for different values of μ^* and dh/dt

	$dh/dt = 0$		% increase in $\overline{W}$ because of $\mu^* \neq 0$	$dh/dt \neq 0$		% increase in $\overline{W}$ because of $\mu^* \neq 0$
	$\mu^* = 0$	$\mu^* \neq 0$		$\mu^* = 0$	$\mu^* \neq 0$	
k_1=k_2=0.0001	0.0387679	0.2024584	422.23%	0.0408690	0.204559	400.52%
k_1=k_2=0.01	0.0019198	0.1656103	8526.43%	0.0024087	0.166099	6795.8%

IV. CONCLUSION

Theoretical investigation of a slider bearing with its stator having a parabolic pad surface and double porous layer attached to the slider, using a ferrofluid lubricant under the presence of magnetic field oblique to the lower surface is represented for its optimum performance. Based on the results obtained from the analysis, the following conclusions are made.

— From equation (8), it can be seen that the constant magnetic field does not enhance $\overline{W}$ in this model.

— With the increase of squeeze velocity, $\overline{W}$ increases in all cases; i.e. whether $k_1 < k_2$, $k_1 > k_2$ and $k_1 = k_2$.

— $\overline{W}$ increases for both $dh/dt = 0$ and $dh/dt \neq 0$ when $k_1 = k_2 = 0.0001$ as compared to $k_1 = k_2 = 0.01$.

— By swapping the widths of upper and lower porous layers does not affect $\overline{W}$, when $k_1 = k_2 = 0.01$ where $dh/dt = 0$ and $dh/dt \neq 0$.

— When the permeability of the upper porous layer is small as compared to lower porous layer, $\overline{W}$ increases with the increase of width of upper porous layer. Similarly, when the permeability of the lower porous layer is small as compared to upper porous layer, $\overline{W}$ increases with the increase of width of lower porous layer.

— Better load capacity $\overline{W}$ is obtained, when width l_1 of upper porous layer and width l_2 of lower porous layer is small for both $dh/dt = 0$ and $dh/dt \neq 0$.

— Both non-dimensional film pressure $\overline{p}$ and load capacity $\overline{W}$ increases significantly with the increase of external magnetic field strength.

— Non-dimensional load capacity $\overline{W}$ increases with the increase of non-dimensional magnetization parameter and the decrease of non-dimensional slip parameter.

V. LIMITATION AND FUTURE SCOPE

The roughness effects are neglected in the present analysis. In the future studies, present model can be analyzed for Shliomis and Jenkin's models of ferrofluid lubrication. Also, this research paper helps engineers to design efficient bearing systems.

Conflict of Interest. The authors declare that there is no conflict of interest.

VII. ACKNOWLEDGEMENT

Authors are grateful to the reviewers for their valuable comments.

REFERENCES

[1]. Morgan, V.T. and Cameron, A. (1957). Mechanism of lubrication in porous metal bearings. *Proc. Conf. on Lubrication and Wear*, London, Institution of Mechanical Engineers, 151-157.

[2]. Prakash, J. and Vij, S.K. (1973). Hydrodynamic lubrication of a porous slider. *J. Mech. Eng. Sc.*, *15* : 232-234.

[3]. Murti, P. R. K. (1975). Squeeze film behaviour in a spherical porous bearing. *Transactions of the ASME*, *97*(4): 638-641.

[4]. Uma, S. (1977). The analysis of double-layered porous slider bearing. *Wear*, *42*: 205-15.

[5]. Naduvinamani, N.B., Santosh, S. (2011). Micropolar fluids squeeze film lubrication of finite porous journal bearing. *Tribology International*, *44*: 409-416.

[6]. Rosensweig, R. E. (1985). *Ferrohydrodynamics*. New York, Cambridge University Press.

[7]. Goldowsky, M. (1980).New methods for sealing, filtering, and lubricating with magnetic fluids. *IEEE transactions on Magnetics*, *16*(2): 382-386.

[8]. Bashtovoi, V. G. and Berkovskii, B.M. (1973). Thermomechanics of ferromagnetic fluids. *Magnitnaya Gidrodinamika*, *3*: 3-14.

[9]. Popa, N.C., Potencz, I., Brostean, L. and Vekas, L. (1997). Some applications of inductive Transducers with magnetic fluids. *Sensors and Actuators*, A *59*: 197-200.

[10]. Mehta, R.V. and Upadhyay, R.V. (1999). Science and technology of ferrofluids. *Current Science*, *76* (3):305 - 312.

[11]. Agrawal, V. K. (1986). Magnetic fluid based porous inclined slider bearing. *Wear*, *107*: 133-139.

[12]. Prajapati, B. L. (1995). Magnetic fluid based porous squeeze films. *J. Magn. Magn. Mater*, *149*: 97-100.

[13]. Ram, P. and Verma, P. D. S. (1999). Ferrofluid lubrication in porous inclined slider bearing. *Indian Journal of Pure & Applied Mathematics*, *30*(12): 1273 - 1281.

[14]. Sparrow, E. M, Beavers, G.S., Hwang, I.T. (1972). Effect of velocity slip on porous walled squeeze films. *J. of lubr. Techno.*, *94*(3):260-264.

[15]. Prakash, J. and Vij, S.K. (1974). Analysis of narrow porous journal bearing using Beavers – Joseph criterion of velocity slip. *Journal of Applied Mechanics*, *41*(2): 348-54.

[16]. Patel, K. C. and Gupta, J. L. (1983). Hydrodynamic lubrication of a porous slider bearing with slip velocity. *Wear, 85*: 309-317.

[17]. Shah, R. C. and Bhat, M. V. (2005). Lubrication of porous parallel plate slider bearing with slip velocity, material parameter and magnetic fluid. *Ind Lubr Tribol*, *57*(3): 03-106.

[18]. Ahmad, N. and Singh, J. P. (2007). Magnetic fluid lubrication of porous-pivoted slider bearings with slip velocity. *Proc I mech E Part J: J Engineering Tribology*, 221: 609 - 613.

[19]. Shah, R. C., Parsania, M. M., Kataria, H. R. (2012). Lubrication of isotropic permeable porous inclined slider bearing with slips velocity and squeeze velocity. *Am. J. Fluid Dyn.*, *2*(4): 61-64.

[20]. Shah, R. C. and Patel, D. B. (2013). Mathematical analysis of newly designed ferrofluid lubricated doubled porous layered axially undefined journal bearing with anisotropic permeability, slip velocity and squeeze velocity. *International J. of Fluid Mechanics Research*, *40*(5): 446-454.

[21]. Shah, R. C. and Kataria, R. C. (2014). Mathematical Analysis of newly designed two porous layers slider bearing with a convex pad upper surface considering slip and squeeze velocity using ferrofluid lubricant. *International journal of Mathematical modeling and computations*, *4*(2): 93-101.

[22]. Shah, R. C. and Patel, D. A. (2016). On the ferrofluid lubricated squeeze film characteristics between a rotating sphere and a radially rough plate. *Meccanica*, 51(8):1973-1984.

[23]. Shah, R. C., Patel, D. A., Kataria, R. C. (2019). Ferrofluid lubricated porous squeeze film bearing with the modified condition of pressure continuity at the film porous interface. *Tribology Online*, *34*(3): 123-130.

[24]. Shah, R. C., Bhat, M. V. (2003). Ferrofluid lubrication equation for porous bearing considering anisotropic permeability and slip velocity. *Indian Journal of Engineering & Materials Sciences*, *10*: 277-281.

[25]. Shah, R. C. and Bhat, M. V. (2003). Effect of slip velocity in a porous secant-shaped slider bearing with a ferrofluid lubricant. FIZIKA A-ZAGREB, *12* (1): 1-8.

[26]. Lin, J. R. and Lu, Y. M. (2004). Steady-state performance of wide parabolic-shaped slider bearings with a couple stress fluid. *Journal of Marine Science and Technology*, *12*(4): 239-246.

[27]. Cameron, A. (1981). *Basic Lubrication theory*, 3rd edition. Ellis Horwood Limited.

How to cite this article: Patel, D. A. and Kataria, R. C. (2020). Characteristics of Double-porous Layered Slider Bearing with Parabolic Pad Stator using Ferrofluid Lubricant. *International Journal on Emerging Technologies*, *11*(2): 1054–1060.